www.acsanm.org Article

Plastic Composites from Repurposed Poly(ethylene terephthalate) Wasted Functionalized Graphene Oxide through Dynamic **Depolymerization**

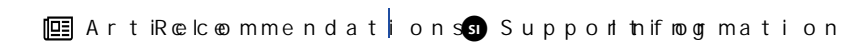
Walker M. Vickery, Katie Lee, Su Min Lee, Jason D. Orlando, and Stefanie A. Sydlik*



Cite This: ACS Appl. Nano Mater. 2024, 7, 3691-3701



ACCESS Lill Metr&Mosre



ABSTRACT: Plastic upcycling, which involves making plastic-derived products with unique or improved properties from discarded plastic materials, is a promising alternative to recycling and disposal to help reduce the overall production of waste. However, recycled and reused materials typically have inferior mechanical, thermal, optical, and barrier properties compared with virgin plastics. Upcycled plastic materials could improve these properties while addressing future waste



accumulation. In this study, we use waste poly(ethylene terephthalate) (PET) collected from disposable food packaging to create a repurposed plastic graphene oxide (GO) composite with a goal of upcycling. We developed a one-pot "dynamic depolymerization" to break down PET in the presence of GO and successfully enabled transesterification of the polymer onto GO. Covalent attachment of PET onto GO and tailorable plastic content was confirmed by thermogravimetric analysis, Fourier transform infrared spectroscopy, X-ray photoelectron spectroscopy, and scanning electron microscopy. These covalent composites (PET-GO) were found to be relatively impermeable to water vapor, showing promise for applications in packaging materials. Aqueous degradation experiments on the composite materials demonstrated that, in bulk conditions, PET-GOs remain mechanically robust while in contact with water over appropriate time scales for packaging applications, while beginning to break down in accelerated conditions. The use of depolymerization methods to promote polymer grafting concurrently with polymer deconstruction could provide a more general method for grafting waste polymers onto oxidized carbonaceous substrates with further study.

KEYWORDS: graphene oxide, upcycling, depolymerization, poly(ethylene terephthalate), composite

INTRODUCTION

Petroleum-based plastics are widely used for their mechanical strength, hydrophobicity, and low permeability to water vapor and oxygen. 1-3 Unfortunately, it is these exact properties that cause common commodity plastics to persist for decades and even centuries in the environment after their disposal.⁴ The proliferation of large-scale plastic waste in the environment can lead to disastrous consequences for aquatic fauna by ingestion or asphyxiation. In addition to the problems caused by large plastic pollutants, the byproducts of plastic degradation and erosion, namely, microplastics, can cause deleterious effects on the Earth.6,7

Recent advances in plastic recycling and upcycling have aimed to address these problems and provided an array of promising technologies for producing usable products from plastic waste.^{8,9} Upcycling of plastic waste involves the use of post-consumer plastic materials as reagents for the preparation of value-added products from waste, most of the resulting products are either new polymers, monomers, or polymer additives. 10 Recycling techniques generally involve producing new plastics from pre-existing post-consumer plastic waste. Among these recycling techniques, pyrolysis 11 and melt processing⁸ are the most commonly used, but they often fail to produce materials with mechanical properties similar to virgin plastics. Newer methods include solvent casting^{9,12} and

depolymerization 13-15 which are capable of producing materials with retained properties but require large amounts of nongreen solvents and expensive catalysts, respectively, depending on the polymer used. While each of these methods has its own benefits and drawbacks, they are inherently limited by the difficulties of the recycling process. Reports from the EPA in 2018 indicated an 8.7% plastic recycling rate in the USA, a number that they have predicted has dropped to between 5 and 6% in 2021 due to changes in global policy on accepting plastic exports from the USA. 16 This number could likely be improved, as a good portion of the collected waste is not suitable for current recycling methods due to the use of polymer blends, additives, and improper cleaning of plastic waste.

Biodegradable and biosourced polymers would help alleviate the burden of plastic contaminants in aquatic and terrestrial ecosystems. Plastics that are capable of expedited degradation

Received: October 26, 2023 Revised: January 19, 2024 Accepted: January 24, 2024 Published: February 9, 2024





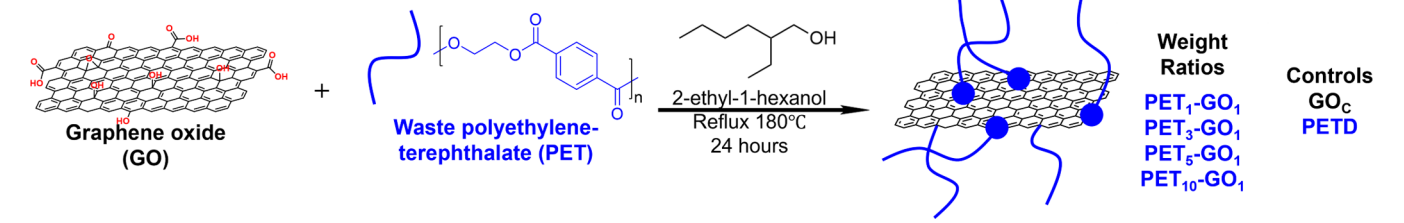


Figure 1. Schematic of the PET-GO attachment process in which GO and PET are covalently attached using 2-ethyl-1-hexanol as a depolymerization reagent. The depolymerization process produces PET oligomers, which are susceptible to chemical exchange with the oxygen functional groups on the surface of GO. Different weight ratios of PET to GO were used to prepare these nanocomposites for further testing and characterization.

into small organic molecules are attractive. Recent works have been able to create biodegradable plastics with mechanical and thermal properties similar to virgin petroleum plastics, such as a vanillin-based thermoset, made by Ma et al. with tensile strength only ~0.4 GPa lower than an epoxy thermoset. 17-19 A continuing problem for such biodegradable plastics is the loss of barrier properties due to the relative hydrophilicity of these polymers often requiring polymer blends or additives, which can introduce their own difficulties. However, recent progress has been made to improve these properties, such as a study by Sangroniz et al. using ring-fused γ -butyrolactone copolymers to make plastics with lower permeability to water, CO₂, and O₂ than poly(methyl methacrylate) and achieving barrier properties similar to those of PET. 20,21 Difficulties could come from finding reliable waste streams that can be used as monomer sources that do not put additional strain on agricultural resources.2

Biodegradable composites are an often overlooked method of expediting degradation. The creation of biodegradable fillers could offer significant advantages, because the inclusion of these additives could expedite the breakdown of macroscopic plastic pollution. Furthermore, approaching plastic degradation by using biodegradable fillers is appealing since fillers can be used in a wide variety of plastics as long as they are miscible in processing conditions, allowing for the simple and easy incorporation of additives. An appropriately engineered additive may also be able to enhance other properties of the plastic that it is incorporated into. One emerging, promising option is the addition of starch, but the efficacy in enhancing degradation of large-scale plastic waste is under scrutiny.^{23–28} In some reports, starch tends to reduce the mechanical strength and barrier properties of plastics leading to continued research into better alternatives. 26 It should also be noted that expedited degradation of large-scale microplastic may lead to an increase in the rate of micro- and nanoplastic production in the short term. Thus, current options for industrial grade biodegradable plastic fillers have much room for improvement, and a tailored filler material may have a great impact on the prospects of plastic degradation. Biodegradable fillers that can enhance the strength and impermeability of plastics would be desirable additives for all plastics and provide a new avenue for the breakdown of plastic. This uniquely positions upcycled fillers to be used in conjunction with future advances in plastic recycling and degradation. Graphene oxide (GO) could be an ideal basis for such a filler.

GO is the oxidized form of graphite, which is a naturally abundant carbonaceous material. GO has a plethora of oxygen functionalities allowing for chemical incorporation and innate aqueous degradability into humic acid-like compounds.²⁷ Additionally, incorporation of GO has been shown to enhance

a variety of physical properties, including mechanical strength and barrier properties, of admixed plastics that they have been incorporated into.^{3,29–32} While these properties make GO an excellent candidate for a biodegradable composite material for plastic fillers, the mechanical strength of the resulting nanocomposites could be further improved through the covalent grafting of polymers to GO. Polymer-functionalized GO allows for mechanical entanglement of the composite with the rest of the polymer matrix, reducing slippage at the polymer-GO interface and eliminating the need for surfactants to disperse the additive. 33,34 Thus, with these design principles in mind, we sought to make a plastic-grafted graphenic material by upcycling plastic waste that could be used for altering the properties of plastic admixtures. Such a plastic-grafted graphenic material would serve as a proof of concept for repurposing waste polymers to create a filler material with potential to be used in virgin or recycled polyesters, including many biobased or biodegradable polyesters to enhance their mechanical, barrier, or possibly biodegradation properties. Plastic-grafted GO that meets these design principles would be a superior option to any currently available.

The synthesis of an upcycled plastic composite consisting of poly(ethylene terephthalate) (PET) grafted-onto GO was conducted by the concurrent depolymerization of waste PET in the presence of GO. Polyesters, such as PET, can undergo depolymerization or transesterification through hydrolysis, 13,35 alcoholysis, ^{36–38} and chemical exchange in a polymer melt ^{8,39,40} typically with the aid of a catalyst. ^{14,36,41} We chose a simple alcoholysis using a bulky alcohol since it typically produces longer oligomers rather than favoring complete depolymerization. In the presence of the alcohol and carboxylic acid groups on GO, acyl substitutions can occur between the PET oligomers and GO. Here, we use "dynamic depolymerization" to depolymerize waste polymers in the presence of GO to achieve covalent attachment and create a repurposed value-added composite material that could serve as a filler for enhancing PET plastic admixtures. We also demonstrate the oxidization and water uptake of the PET-GO composites in aqueous conditions over time, with higher plastic content composites demonstrating greater resistance to chemical change.

RESULTS AND DISCUSSION

Synthesis. Dynamic depolymerization of PET onto GO was achieved using a bulky alcohol which serves as a transesterification reagent.¹³ Other alcohols, such as ethylene glycol and cresols have been observed to break down PET through alcoholysis. 42,43 2-Ethly-1-hexanol was chosen for its

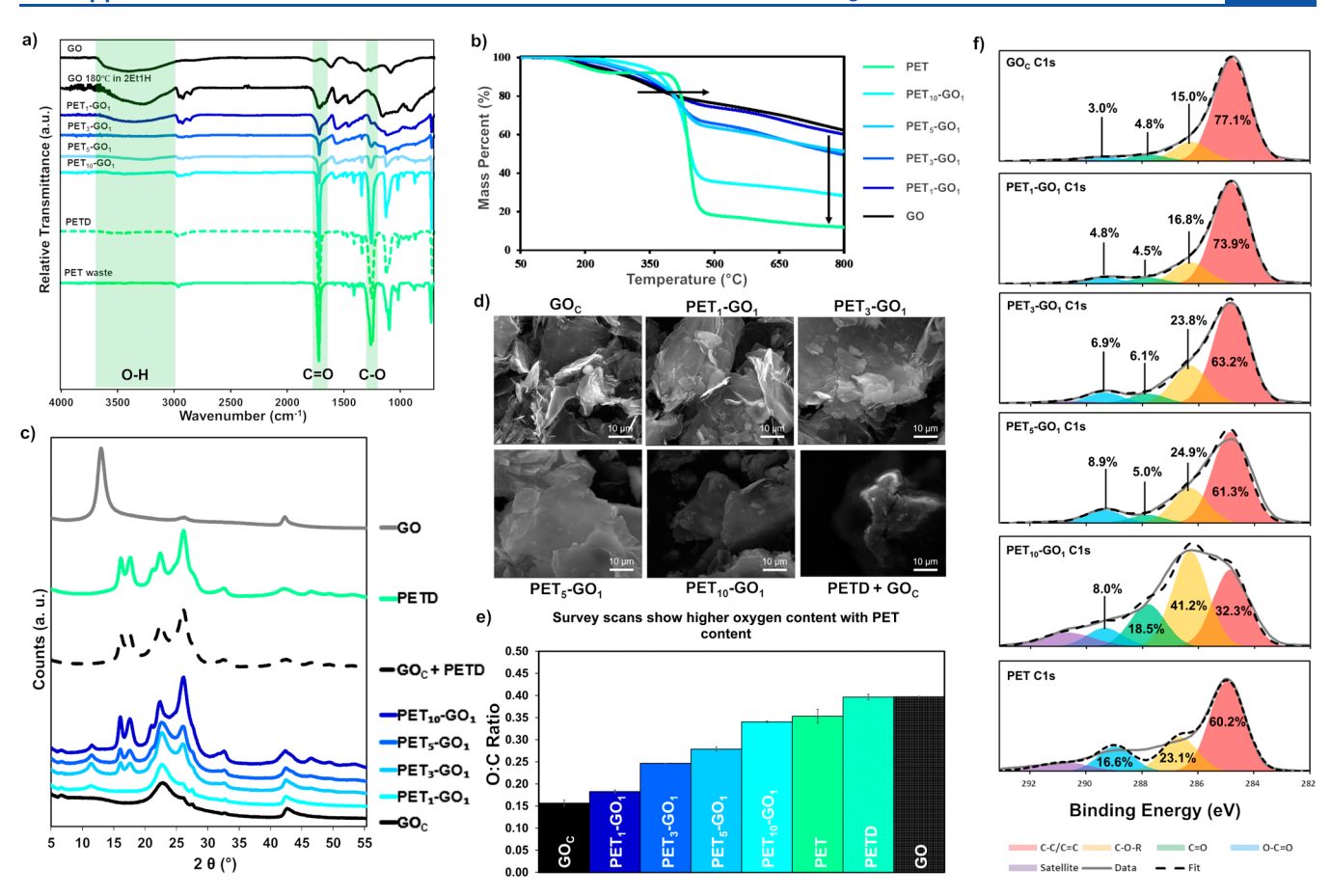


Figure 2. (a) FTIR of PET-GO materials and controls show loss of alcohol stretch from covalent attachment and increasing carbonyl stretching modes. (b) Thermograms, char weights, and onset temperatures for PET-GO materials and controls, including an admixed control, demonstrating shifts in thermal properties depending on PET content. (c) XRD of PET-GO weight ratios shows a unique 2 θ peak that is present as more PET is added to the reaction. This unique peak is not observed in a control admixture. d-Spacings of major peaks: 7.71, 5.51, 5.04, 3.96, 3.40, 2.74, and 2.13. (d) SEM of PET-GO materials. (e) Samples of deconvoluted C 1s high-resolution XPS scans with averaged atomic percent values from 3 spot scans displayed. (f) XPS survey scans showing the ratio of carbon to oxygen based on atomic %.

ability to break down PET into oligomers, and m-cresol had been used as the bulky phenol in earlier attempts with no success. Varying weight ratios of GO were used to target composites with a mass composition of 1:1, 3:1, 5:1, and 10:1 $\rm PET_{x^-}GO_y$ (PET_1-GO_1, PET_3-GO_1, PET_5-GO_1, and PET_10-GO_1, respectively), where PET_10-GO_1 targets the highest PET incorporation. PET used in these experiments was collected directly from consumer food package waste. To prepare for the chemical reaction, PET from clear food-grade packaging was thoroughly washed with soap and water and mechanically processed into flakes smaller than 1 cm².

In a typical dynamic depolymerization experiment, PET flakes from waste plastic (1.0, 3.0, 5.0, or 0.1 g), GO (0.1 g), and 2-ethyl-1-hexanol (15 mL) were added to a flame-dried round-bottom flask, fitted with a reflux condenser, and allowed to react at 180 °C and left refluxing over 24 h (Figure 1). The product was a murky, gray suspension which was filtered and washed with methanol before drying on vacuum overnight. A more detailed description of the synthetic protocol can be found in the Supporting Information (SI). Two controls were prepared in which GO or PET were omitted from the reaction to prepare a heated and reduced GO sample (GO_C) or depolymerized PET oligomer (PETD), respectively. PETD is used as a control to account for properties from the PET-GO materials that may be due to the presence of a PET oligomer.

It is also being used to serve as an approximation for end-of-life recycled PET.

Characterization. Fourier Transform Infrared (FTIR) Spectroscopy. The chemical composition of the prepared PET-GO composite materials was first characterized by using FTIR to observe the chemical bonds present. Neat PET is characterized by a C=O ester stretch appearing at 1720 cm $^{-1}$. PETD shows similar stretching modes with a minor increase in the C-H stretch region of ~2900-3000 cm⁻¹ and a new peak at 1340 cm⁻¹ which is being attributed to a new aromatic ester C-O stretching mode from the alcoholysis. When PET-GO is prepared, this characteristic PET peak appears at 1717 cm⁻¹ which is indicative of PET present with the GO sheet. Similarly, the aromatic ester peak exhibited by esters at 1254 cm⁻¹ is present in the PET-GO materials. The intensity of both peaks increases with increasing incorporation of PET, with PET₁₀-GO₁ including the highest amount of PET and correspondingly the most intense ester peaks (Figure 2a). Most indicative of increasing PET content is that these characteristic PET peaks increase relative to a GO_C characteristic C=C stretching mode, at 1554 cm⁻¹ in the higher weight ratio PET-GOs. Interestingly, the broad O-H stretching peak in the 3500–3000 cm⁻¹ region is present at lower weight ratios of PET to GO but nearly disappears by the PET₃-GO₁ ratio, suggesting that at higher weight ratios, nearly all of the

carboxylic acid or alcohol functional groups on GO that are not being thermally reduced are reacting with PET oligomer on the GO.

Thermogravimetric Analysis (TGA). Increasing amounts of covalently bound PET were further corroborated by shifts in the material onset temperatures and char weights in TGA (Figure 2b). Thermograms confirmed that increased polymer content was achieved by increasing the amount of PET in the reaction, with PET₁₀-GO₁ having the lowest char weight at 28.2% and an onset temperature of 397.4 °C, which are the closest to those of waste PET. The char weights of GOC PET₁-GO₁, PET₃-GO₁, PET₅-GO₁, PET₁₀-GO₁, and PET are 62.11, 60.13, 49.45, 51.40, 28.18, and 11.86 mass percent, respectively. These char weights can be used to estimate the loading efficiency of the PET-GO reaction for each PET-GO composite by using the char weights of PETD and GOC, the component parts of PET-GO. These estimates showed that PET₁₀-GO₁, PET₅-GO₁, PET₃-GO₁, and PET₁-GO₁ contained 62.04, 19.57, 23.16, and 3.62% PETD by mass, respectively (SI, page S27). Thus, PET-GOs have attachment efficiencies of approximately 16.3, 4.9, 10.0, and 3.8% of the added PET for PET₁₀-GO₁, PET₅-GO₁, PET₃-GO₁, and PET₁-GO₁, respectively. While this is not a large portion of the overall plastic used, we still are able to get a high degree of functionalization through this method. One could easily imagine sequestering the remaining mass of PET for other purposes.

The higher onset temperatures of PET-GOs, when compared to GO_C, suggest PET attachment to the more facile GO leaving groups, causing them to become more thermally stable. Onset temperatures for GO_C, PET₁-GO₁, PET₃-GO₁, PET₃-GO₁, PET₃-GO₁, and PET are 208, 231, 329, 346, 397, and 416 °C, respectively. Additionally, when a PET₁₀-GO₁ sample was heated in nitrobenzene at 180 °C for 1 h and filtered hot to remove any noncovalently bound PET oligomer, the change in onset temperature and char weight of the sample before and after the wash was negligible, indicating successful covalent attachment (Figure S16). If any noncovalently bound polymer was present, it would have been washed away and a significant change in TGA char weight would have been seen.

Differential Scanning Calorimetry (DSC). Melting point $(T_{\rm m})$ and glass transition temperature $(T_{\rm g})$ assessments were performed on a representative set of PET, PETD, PET₁₀-GO₁, PET₁-GO₁, and the noncovalently mixed PETD and GO_C (Figures S23 and S24). Glass transition temperatures, typically seen around 80-90 °C for PET, were largely suppressed in all materials, which is typical of polymer-grafted materials. The suppression of the T_g in the PET waste can be attributed to additives commonly used to prevent plastic deformation in commercial sources of PET. The melting point isotherm indicative of PET reduced from 246 °C for the noncovalent mixture, to 239 and 240 °C for PET₁₀-GO₁ and PET₁-GO₁, respectively. The reduced melting point in the PET-GO materials could be an indicator of covalent attachment since covalently bound PET oligomers would inevitably exhibit different molecular dynamics than free polymers.

X-ray Diffraction (XRD). The emergence of a new 2θ peak in the XRD spectra of all of the PET-GO materials demonstrates a change in interlayer spacing, found using Bragg's Law, that is not present in noncovalent mixed controls (Figure 2c). The new peak at 11.9° is indicative of an interlayer d-spacing of around 7.4 Å. While a similar signal is typical of GO at interlayer d-spacing of GO, at 6.8 Å (2θ of 12.9°), this interlayer spacing is lost due to the intense heating of the

reaction conditions.⁴⁴ Typically, when thermally reduced, the interlayer spacing of GO shrinks to 3.9 Å ($2\theta = 22.7^{\circ}$) due to loss of chemical functionalities. Thus, the fact that this signal at 11.9° in the PET-GO materials is present rather than lost to reduction suggests covalent attachment of oligomeric chains.⁴⁵

Scanning Electron Microscopy (SEM). The covalent attachment of PET to GO was further supported by SEM images of PET-GO materials (Figure 2d). Electrically insulating materials, like PET, will charge when subject to the secondary electrons of the SEM which produces lower contrast in areas of the image that are more insulating. 46 Thus, as the PET content was increased from GO_C to PET₁₀-GO₁ there is a trend toward darker contrast. Furthermore, the noncovalent control of dry-mixed PETD and GO_C shows that there are still areas of brighter contrast expected of a highly conductive reduced graphenic basal plane; none of these bright spots are visible in the covalently attached PET₁₀-GO₁ demonstrating a more homogeneous surface due to direct covalent attachment. Altogether, PET-GO exhibits a more homogeneous surface chemistry than the noncovalent mixture suggesting attachment.

X-ray Photoelectron Spectroscopy (XPS). PET content and the nature of the covalent attachment were investigated by survey and high-resolution XPS scans. Survey scans of the various PET-GO materials shows that higher PET-to-GO weight ratios have a higher atomic percent oxygen with PET₁₀-GO₁ having 25.4% O compared to GO_C with 13.5% O (Figure 2e). Additionally, the C and O contents of neat PET waste and depolymerized PET oligomer were similar to very little change in chemical composition due to the depolymerization process. This suggests oligomer formation rather than complete degradation into monomeric units, which would have an expected C:O ratio of 6 rather than 2.5 (calculations in the SI).

High-resolution C 1s scans of the PET-GO materials demonstrate an increase in the relative amount of ester and ether groups with an increase in PET content (Figure 2f). This increase is in good agreement with greater PET content seen in FTIR and TGA. When compared to a noncovalent control (Figure S20), which was prepared by dry mixing depolymerized PETD plasticizer with $GO_{\rm C}$ in a 10 to 1 weight ratio, PET_{10} -GO₁ has a 12.5% increase in the number of ester functional groups present. High-resolution scans of the noncovalent control have greater error than the PET-GO samples, an indication that it has a less homogeneous composition compared to the covalent attachment methods.

Dynamic Light Scattering (DLS). PET and PETD polymer length was estimated using DLS to predict the polymer length. This was the method of choice due to the ability to use TFA as the solvent system, which dissolves PET at room temperature. PET was estimated to have an average molecular weight of 178.3 kDa that would be approximately 929 repeat units long. PETD was found to have an average molecular weight of 16.1 kDa that would be approximately 84 repeat units long, a nearly 11-fold decrease in size. This suggests that 16.1 kDa is the average molecular weight of PET oligomers attached to PET-GO materials.

A representative set of PET₁₀-GO₁, GO_C, and noncovalently mixed PETD and GO_C were dispersed in TFA and analyzed for their Z-average size. GO_C and the noncovalent mixture exhibited similar Z-average sizes of 5131 and 5605 nm, demonstrating the minimal effect that PET adsorbed to the graphenic basal plane has on the particle size. Interestingly, the PET-grafted GOs demonstrated much larger particle sizes in

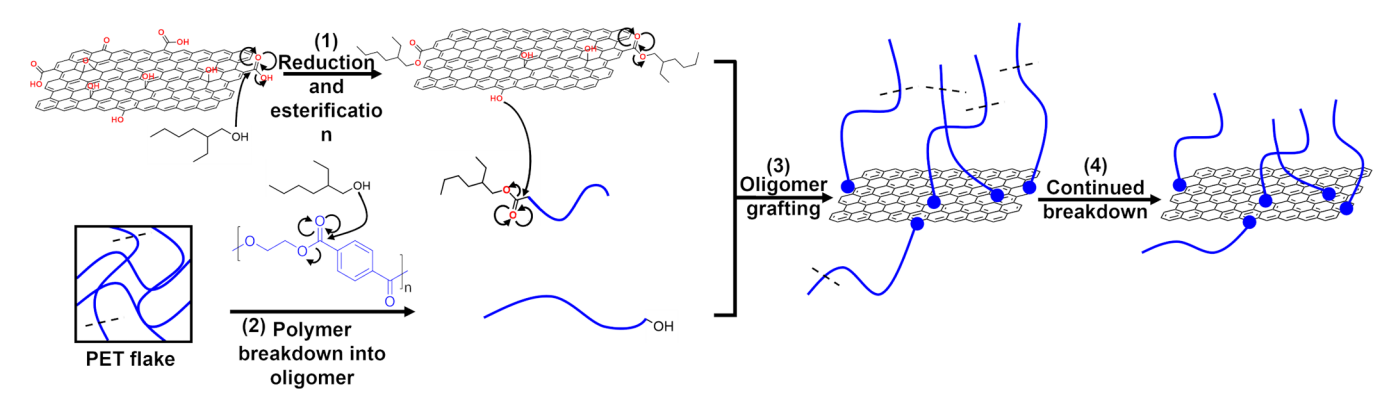


Figure 3. Hypothesized mechanism of dynamic depolymerization of PET onto GO through transesterification between oligomers and chemical functional handles on the surface of GO.

DLS of 17310, 4154, 5909, and 2696 nm for PET $_{10}$ -GO $_{1}$, PET $_{5}$ -GO $_{1}$, PET $_{3}$ -GO $_{1}$, and PET $_{1}$ -GO $_{1}$, respectively (Chart S1). This increase in particle size with greater PET attachment is further evidence of the covalent grafting of PET to GO. The standard deviations in particle size for PET $_{5}$ -GO $_{1}$ and PET $_{3}$ -GO $_{1}$ overlap, so size estimates are not statistically significant. Interestingly, PET $_{1}$ -GO $_{1}$ has a smaller particle size than the GO $_{C}$ -based controls, the authors attribute this decrease in size to the improved dispersibility of PET $_{1}$ -GO $_{1}$ in TFA while having a relatively low PET grafting amount that does not appreciably increase flake size.

Proposed Mechanism of Dynamic Depolymerization. We predict that the dynamic depolymerization of PET onto GO proceeds in the following manner (Figure 3). (1) Initially, graphene oxide begins to be thermally reduced at the high reaction temperatures, while 2-ethyl-1-hexanol reacts with carboxylic acid functionalities on GO to form esters, leaving primarily alcohol containing functional groups on the surface of GO. (2) PET backbone is broken down into PET oligomers by the bulky alcohol starting from the surface of the flakes, forming longer plastic chains. PET oligomers continue to depolymerize in solution. (3) Transfer occurs between alcohols on the surface of GO and free PET oligomers through transesterification, leading to covalent grafting of PET onto GO. (4) If the reaction is allowed to proceed, covalently attached PET chains can continue to depolymerize slowly until the temperature is reduced and the reaction is stopped.

- (1) The mechanism of this dynamic depolymerization reaction was hypothesized based on evidence from FTIR, TGA, and XPS of the PET-GOs and their controls. In the control where GO and 2-ethyl-1-hexanol were refluxed at 180 °C, GO was thermally reduced over the course of the reaction based on XPS elemental analysis (Figure 2d). Alcohols were the main oxygencontaining functional group remaining after thermal reduction based on high-resolution C 1s XPS deconvolution. A fair number of carboxylic acid/ester groups also remained which were likely carboxylic acid functional groups that were esterified by 2-ethyl-1hexanol, as suggested by FTIR. FTIR corroborates this claim as a new C-H stretching mode at ~2900-3000 cm⁻¹ attributed to the aliphatic portion of 2-ethyl-1hexanol appear (Figure 2a).
- (2) PET flakes began the reaction as a heterogeneous suspension. Throughout the course of the reaction, these

flakes were observed to turn from clear to opaque on the surface and would slowly shrink as the reaction progressed. This is in accordance with observations found in the literature. 47,48 This allows us to hypothesize that PET oligomers were likely formed by breaking down polymer chains on the surface of the waste. It is these PET oligomers that are released from the surface of flakes that are free in solution to react on the surface of GO to form covalent bonds through chemical exchange. These bonds are likely formed through the alcohol functional groups on GO since they are the only nucleophile available that can undergo transesterification reactions with PET oligomers.

- (3) Successful grafting of PET oligomers onto GO was established by FTIR, TGA, XPS, XRD, and SEM in the above characterization sections. For GO to interact with the PET oligomers, they would have to be free floating in the reaction mixture with each other.
- (4) After 12 h of reaction, a maximum PET functionalization and length were achieved. To determine this, we ran several time trials for each weight ratio and analyzed the resulting powders via FTIR and TGA. By 3 and 6 h of reaction time, significant amounts of solid PET flakes were still present in the reaction mixture. As the reaction progressed through 12, 18, and 24 h for each weight ratio, the PET content decreased. This was demonstrated by the TGA onset temperature decreases and an increase in the char weight (Figure S2). Thus, as the reaction proceeded after all of the PET flakes were consumed, the thermal properties of the PET-GO materials began to shift to more closely resemble those of GO_C, suggesting that either PET chains were being cleaved from the GO basal plane or the grafted oligomer chains were shortening as the reaction proceeded.

Shortening of the polymer chains attached to GO was determined to be the pathway for PET reduction. Cleaving the entire polymer chain would involve the transesterification of ester at the GO PET interface, thus creating alcohol groups on the GO basal plane. Because FTIR of these materials shows that the intensity of the O–H stretching mode tended to decrease as the reaction progressed from 12 to 24 h cleavage at the site of polymer conjugation is not likely (Figure S1). Additionally, FTIR revealed that PET chain shortening was occurring, as seen by the gradual decrease in the intensity of the ester stretching mode at 1722 cm⁻¹.

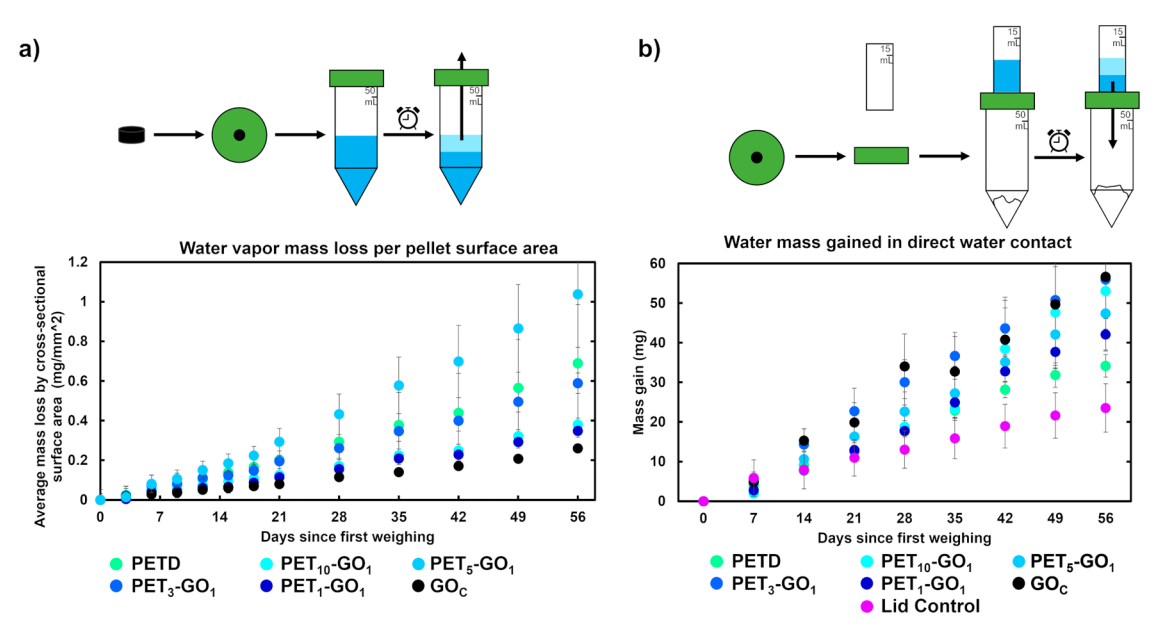


Figure 4. (a) Water vapor and (b) direct water contact permeability through hot-pressed pellets of PET-GO materials and controls, respectively.

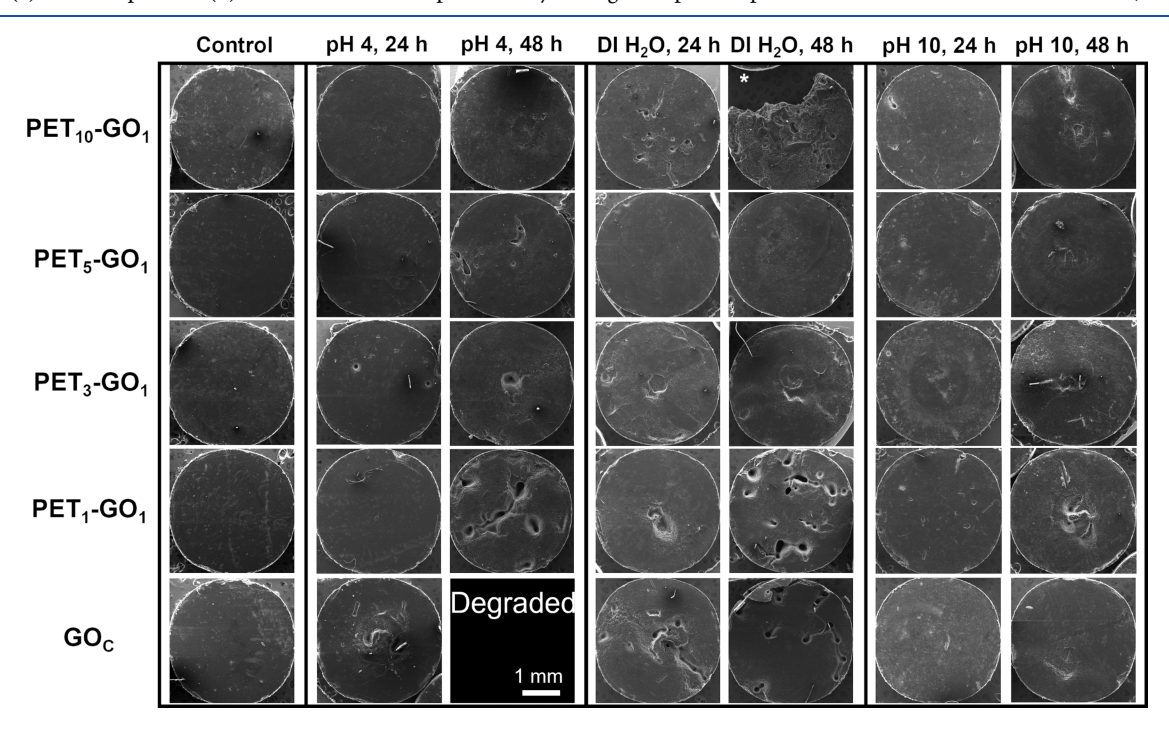


Figure 5. Hot-pressed pellets of composite materials sonicated under acidic, neutral, and alkaline conditions using a bath sonicator for up to 2 days. Higher graphenic content in pellets showed more visible surface damage in materials except in alkaline conditions. * indicates damage caused to PET_{10} -GO₁ sonicating in DI water for 48 h by mechanical sources.

Material Properties. Water Permeability Studies. Water impermeability is necessary for many plastic packaging applications as water vapor can often negatively affect the product. Plastic permeability is only going to become more important as hydrophilic biodegradable plastics begin to see popular use. Graphenic materials have been used as fillers and coatings to reduce the permeability of gas and water vapor in plastic composites due to their planar two-dimensional (2D) structure and impermeability to small molecules.²⁹

To assess the permeability of the bulk PET-GO composites to water vapor, hot-pressed pellets were tested by analyzing mass loss from a closed system due to water evaporation. Hotpressed pellets were prepared as described in the "PET-GO pellet processing" section of SI page S5. Inspired by other experimental set-ups, 49,50 hot-pressed pellets of controls or upcycled PET-GO materials were inserted into centrifuge tube lids and placed on centrifuge tubes filled with $\sim\!20$ mL of deionized (DI) water (Figure 4a). The tubes were sealed with parafilm and weighed for water mass loss from evaporation over a period of 8 weeks to map the relative permeability of each material (more information in the SI).

PET-GO materials were less permeable to water vapor than depolymerized PET (PETD) pellets over an 8-week period, except for PET₅-GO₁ (Figure 4a). Notably, both PET₁-GO₁

ACS Applied Nano Materials

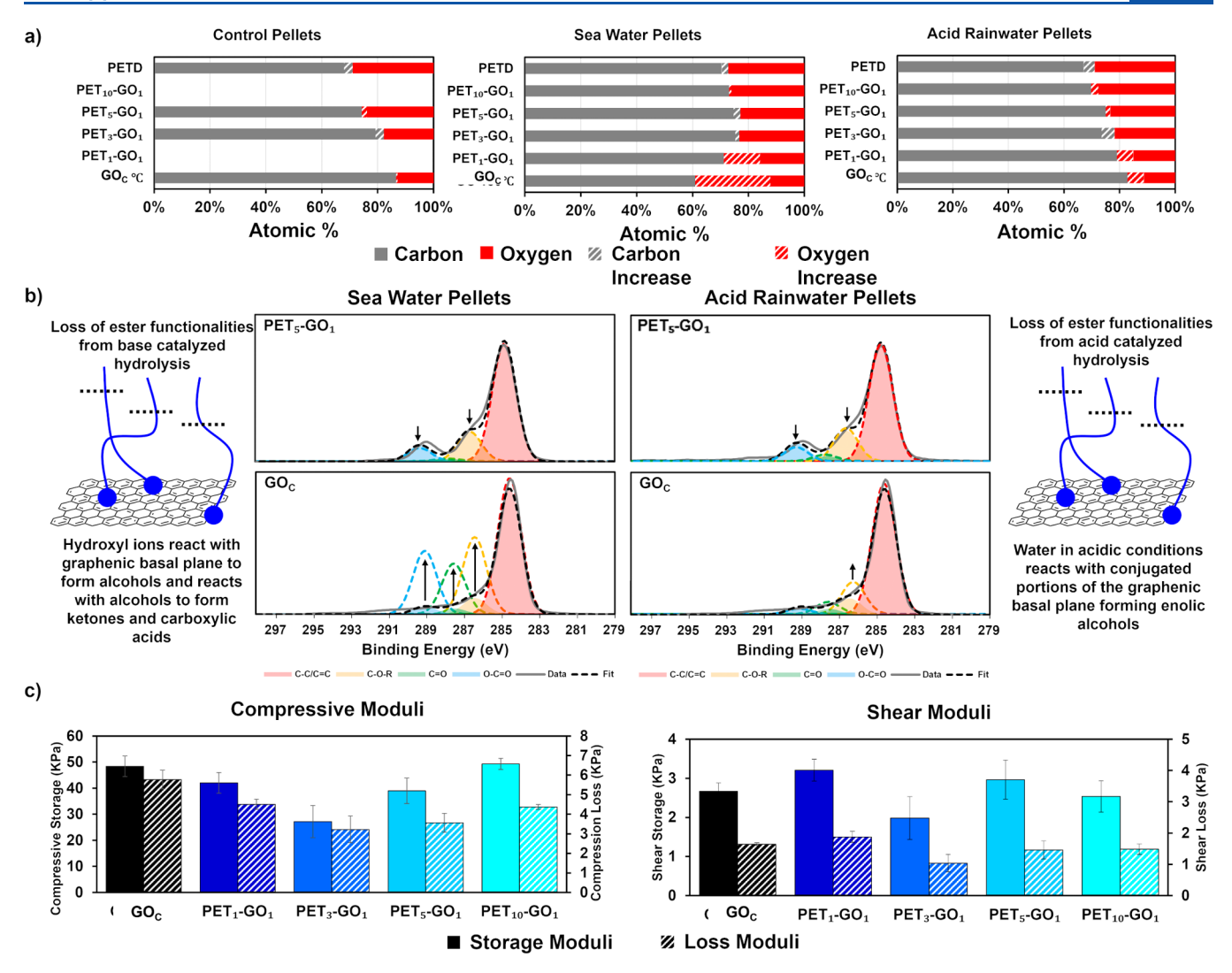


Figure 6. (a) Averaged XPS survey scans for pellets of PET-GO materials aged in air, simulated ocean water, or simulated acid rain. The largest changes were observed in the oxidation of GO_C and PET_1 - GO_1 which were highly oxidized in the simulated ocean water, whereas PET-GOs with a higher PET content were shielded from the bulk of the oxidation. (b) Sample XPS high-resolution scans from the GO_C control and PET_5 - GO_1 demonstrating the major chemical alterations from aqueous conditions over time caused by PET cleavage and GO oxidation. (c) Mechanical tests performed after pellet manufacturing and prior to aging. Little variation was observed in the pellet's mechanical properties over the 12-week period, suggesting a maintenance of good properties for the lifespan of packaging applications (Figures S4–S9).

and PET_{10} - GO_1 had low vapor permeability close to that of the GO_C , with average net water mass losses of 0.348 mg and 0.379 mg per mm² of cross-sectional pellet area, respectively, over the 8-week period, suggesting these materials as good candidates for future permeability testing in plastic films.

An alternative permeability setup was also designed in which water was in direct contact with the pellet surface using a reservoir filled with DI water on the outside of the tube (Figure 4b). In these water contact experiments, diffused moisture was captured using CaCl₂ desiccant in a sealed vial, and mass gain was tracked over 8 weeks. Interestingly, the permeability trend observed in the water contact setup appears to be roughly the inverse of that seen in the water vapor diffusion tests (Figure 4b). These paradoxical results can be explained by the physical dimensions and relative hydrophilicity of graphenic materials. The large two-dimensional structure of graphenic materials and high surface area creates a more tortuous path for gaseous molecules, in this case, water vapor, making it more impermeable than many other materials. Since GO-based materials also have oxygen-containing functional groups, it is

also relatively hydrophilic which aids in channeling water when in full contact with the graphenic material and has been observed to aid in promoting capillary action when wetted. 51,52 In general, the PET-GO materials were more permeable than the PETD control, with $\rm GO_{C}$ and $\rm PET_{3}\text{-}GO_{1}$ consistently exhibiting the most water mass gain of any pellet tested. $\rm PET_{10}\text{-}GO_{1}$ showed a similar permeability to the lower PET content materials by the end of the 8 weeks but was generally less water-permeable until week 6.

This suggests not only that these graphenic materials are less permeable to water vapor than the oligomeric control but also that they are more susceptible to environmental degradation upon disposal. These bulk PET-GO properties suggest that future work using these materials as a filler as they relate to permeability should focus on PET₁-GO₁ or PET₁₀-GO₁ since these were generally less vapor permeable while still being highly water-absorbent. This combination of properties is ideal for single-use packaging applications. In these applications, water vapor will not permeate through packaging, keeping food fresh. However, upon disposal, enhanced water permeation in

aqueous conditions may potentially allow for expedited degradation.

Ultrasonic Degradation Study. Bath sonication has previously been used to approximate long-term mechanical weathering.²⁸ Thus, to assess the relative long-term stability of each composite material, an expedited degradation experiment using bath ultrasonication was devised. Acidic, neutral, and alkaline aqueous conditions were used over a period of 2 days to simulate various pH values associated with acid rain, neutral water, and ocean water. The integrity of each pellet was assessed visually by SEM (Figure 5). The controls did not change after being left in air for the 2-day period. For the ultrasonicated pellets, the lower PET content PET-GOs, namely, GO_C PET₁-GO₁, appeared to have more superficial damage. This trend was apparent for the acidic and neutral pH conditions but less so for the alkaline conditions. This enhanced stability of higher-PET-ratio PET-GOs was likely due to the improved surface interactions due to the polymer's ability to entangle or possibly indicative of annealing due to the hot-pressing process.8 It should also be noted that when this test was conducted with PETD pellets, all of the pellets lost shape and degraded into free floating plastic flakes and insoluble plastic residue, highlighting the relative stability of PET-GO materials exposed to mechanical weathering.

Degradation. To assess the long-term degradation, pellets of the graphenic materials were soaked in simulated ocean water and acid rainwater over 12 weeks and compared to pellets left standing in air. 53,54 Pellets were dried and weighed, and the mechanical properties were tested in shear and compression. Pellets gained mass in all aqueous media in the first week after soaking, suggesting rapid water absorption by PET-GO materials (Figure S15). Absorption was greatest in PET₁-GO₁ and the lower PET-GO weight ratios, which is in good agreement with the relative hydrophilicity observed in the water contact permeability tests. After the first week, low PET content materials (PET₁-GO₁, PET₃-GO₁) fluctuated between losing and gaining mass, suggesting that degradation occurs through cycles of water absorption and decomposition, while the higher-PET-content materials (PET₅-GO₁, PET₁₀-GO₁) showed less initial absorption and the weight remained relatively consistent, suggesting higher hydrophobicity.

Mechanical Properties. The bulk mechanical properties of the PET-GO pellets were assessed in terms of shear and compression. High shear and compressive moduli are important characteristics of viable filler materials, and bulk mechanical properties are suggestive of admixture properties. Overall, PET-GO materials showed good mechanical properties, comparable to those of GO (Figure 6c). Because grafted PET enhances miscibility in polymer mixtures, this should allow for better integration of the filler material. Additionally, there is precedent for polymer-grafted graphenic materials enhancing mechanical properties as a filler across a variety of polymers including PET. 33,34,-59 This suggests that these upcycled PET-GO composites are excellent candidates for fillers in consumable plastics.

Changes in the mechanical properties of the bulk pellets were used to help assess the breakdown of the bulk constructs over time in aqueous conditions. The mechanical properties of the pelleted materials were assessed weekly for the first 12 weeks of the pellet degradation experiments to identify trends in mechanical breakdown of the material (Figures S4–S9). It is worth noting that the PETD control pellets were very fragile, with most of them, including the dry control, shattering during

handling as opposed to the more robust graphenic pellets, which remained intact. There is no significant difference in compressive or shear moduli between the control and degraded pellets over time.

XPS of Degraded Pellets. To better understand the chemical changes occurring after aging, PET-GO pellets were characterized via XPS prior to and at the conclusion of the 12week degradation study. Survey scans of the carbon and oxygen contents of the control pellets showed minimal change in the carbon and oxygen contents of the surface of the pellet over time. Small changes in the surface chemistry of the control pellets may be attributed to handling over the 12-week experiment. GO_C and PET₁-GO₁ pellets left soaking in simulated acid rain and ocean water exhibited much more drastic changes to their surface composition, with a net oxygen gain of 5.8 and 5.9% in acidic conditions and 26.9 and 13.0% in ocean water, respectively. In both types of aqueous media, GO_C and PET₁-GO₁ were greatly oxidized demonstrating the lower chemical resistance of the graphenic basal planes that do not have a sufficiently protected plastic-covered surface (Figure 6a). The greater oxygen content at the surface can be attributed to oxidation of the sample surface rather than loss of carbon in the bulk sample, since any weathering would cause exposure of the underlying bulk material, resulting in a C/O ratio more chemically similar to the regular bulk material. 60,61 Furthermore, the degree of oxidation for these materials was greater in the simulated ocean water, which is to be expected in the more alkaline conditions since the GO basal plane is expected to degrade in the presence of hydroxyl ions.²⁷ PET₃-GO₁, PET₅-GO₁, and PET₁₀-GO₁ did not exhibit a large change in the overall oxygen content; however, high-resolution C 1s spectra deconvolution reveals alterations in the type of oxygen-containing functional groups left on the surface.

Simulated ocean water decreased the amount of carbonylbased carbon species present, with the exceptions of GOC and PET₃-GO₁ (Figure 6b). Likewise, simulated acid rainwater similarly decreased the carbonyl content with the exception of PET₁₀-GO₁. This loss of carbonyl groups along with a tendency for the higher PET-to-GO weight ratio materials to have a loss of alcohol functional groups suggests that acid- and base-catalyzed hydrolysis mechanisms are both causing the degradation of the PET chains on these grafted materials consistent with literature depolymerizations. 37,38,62 GO_C served as a control to allow for the observation of chemical changes in the graphenic basal plane throughout aqueous degradation. In the GO_C samples, the mechanism of degradation of the graphenic portion can be observed. For GO_C in simulated ocean water, there was a significant increase in the number of alcohol and carbonyl groups on the surface of the materials, suggesting that hydroxide ions react with GO and oxidize the surface. GOC in simulated acid rain had a loss of carbonyl groups but an increase in the relative number of alcohols. Thus, in acidic conditions, water can interact with the graphenic basal plane to form alcohol functionalities. Both of these are consistent with previous models for the degradation of graphenic materials in aqueous conditions.²

CONCLUSIONS

This paper reports a novel method to graft waste polymers to a substrate through a depolymerization process in a simple one-pot reaction. Successful covalent attachment of PET oligomers to GO has been achieved through a dynamic depolymerization procedure that produces a value-added composite from

upcycled plastic waste. This one-pot grafting-onto process was performed by depolymerizing waste PET in the presence of GO to promote transesterification between the depolymerized oligomer and GO functional groups. Increasing PET content and covalent attachment was verified by FTIR, TGA, XPS, XRD, and SEM. Additionally, FTIR suggests that saturation of GO reactive sites likely occurs at a weight ratio between PET₁-GO₁ and PET₃-GO₁.

PET-GO materials exhibited lower water vapor permeability than the recycled PET control but an increase in permeability when in direct contact with water. This suggests that PET-GO could be an ideal material for disposable food packaging by keeping water vapor out when packaged and accelerating breakdown in aqueous environments upon disposal. PET-GO composite mechanical properties remained consistent with GO suggesting good mechanical properties.

This technique could provide an avenue to produce inexpensive polymer-functionalized materials by using waste plastic and depolymerization catalysts. Immediate next steps include testing the capabilities of this composite as a filler incorporated in plastic films for packaging applications and analyzing any changes in biodegradability based on the composite amount and content. Alternative carbonaceous substrates that can be oxidized, such as activated charcoal, 63 could be tested to expand the scope of this chemistry. Furthermore, the scope of depolymerization reactions can be expanded to include more plastic waste types from other condensation polymers, such as polyurethanes and polyamides. For example, with PET-GO, we have already attempted the simple heating of PET in the presence of GO using hot nitrobenzene as the solvent with some success of attachment. A PET₁₀-GO₁ sample prepared using hot nitrobenzene in this way produced a TGA char weight of 23.2% which would indicate an improved PET loading content compared to that observed with 2-ethyl-1-hexanol; however, we decided to use 2-ethyl-1-hexanol due to its relative toxicity, cost, and its previous use as a depolymerization agent (Figure S18). This technique may renew interest in less efficient depolymerization methods, as depolymerizations that generate oligomers rather than monomers would allow for longer grafted polymer chains. Dynamic depolymerization offers a method for producing value-added materials from waste and presents an exciting new alternative to traditional recycling.

ASSOCIATED CONTENT

Supporting Information

The Supporting Information is available free of charge at https://pubs.acs.org/doi/10.1021/acsanm.3c05131.

All characterization techniques; synthetic methods and characterization data for PET-GO materials; pellet manufacturing; rheological testing; permeability experiments, and control data (PDF)

AUTHOR INFORMATION

Corresponding Author

Stefanie A. Sydlik – Department of Chemistry, Carnegie Mellon University, Pittsburgh, Pennsylvania 15213, United States; oocid.org/0000-0001-9375-2356;

Email: ssydlik@andrew.cmu.edu

Authors

Walker M. Vickery — Department of Chemistry, Carnegie Mellon University, Pittsburgh, Pennsylvania 15213, United States; © orcid.org/0000-0002-5273-137X

Katie Lee – Department of Chemistry, Carnegie Mellon University, Pittsburgh, Pennsylvania 15213, United States Su Min Lee – Department of Chemistry, Carnegie Mellon

University, Pittsburgh, Pennsylvania 15213, United States;
ocid.org/0009-0000-1989-2019

Jason D. Orlando – Department of Chemistry, Carnegie Mellon University, Pittsburgh, Pennsylvania 15213, United States

Complete contact information is available at: https://pubs.acs.org/10.1021/acsanm.3c05131

Notes

The authors declare no competing financial interest.

ACKNOWLEDGMENTS

The authors thank J. Gillespie for providing training and use of the XPS (Materials Characterization Laboratory at the University of Pittsburgh). The authors acknowledge use of the Materials Characterization Facility at Carnegie Mellon University supported by grant MCF-677785. They also thank the Carnegie Bosch Foundation for funding for this project.

REFERENCES

- (1) Aradhana, R.; Mohanty, S.; Nayak, S. K. Comparison of Mechanical, Electrical and Thermal Properties in Graphene Oxide and Reduced Graphene Oxide Filled Epoxy Nanocomposite Adhesives. *Polymer* **2018**, *141*, 109–123.
- (2) Mueller, K.; Schoenweitz, C.; Langowski, H.-C. Thin Laminate Films for Barrier Packaging Application Influence of Down Gauging and Substrate Surface Properties on the Permeation Properties. *Packag. Technol. Sci.* **2012**, 25 (3), 137–148.
- (3) Pinto, A. M.; Cabral, J.; Tanaka, D. A. P.; Mendes, A. M.; Magalhães, F. D. Effect of Incorporation of Graphene Oxide and Graphene Nanoplatelets on Mechanical and Gas Permeability Properties of Poly(Lactic Acid) Films: Incorporation of GO and GNP in PLA Films. *Polym. Int.* **2013**, *62* (1), 33–40.
- (4) Chamas, A.; Moon, H.; Zheng, J.; Qiu, Y.; Tabassum, T.; Jang, J. H.; Abu-Omar, M.; Scott, S. L.; Suh, S. Degradation Rates of Plastics in the Environment. ACS Sustainable Chem. Eng. 2020, 8, 3494—3511.
- (5) Alexiadou, P.; Foskolos, I.; Frantzis, A. Ingestion of Macroplastics by Odontocetes of the Greek Seas, Eastern Mediterranean: Often Deadly! *Mar. Pollut. Bull.* **2019**, *146*, 67–75.
- (6) Boots, B.; Russell, C. W.; Green, D. S. Effects of Microplastics in Soil Ecosystems: Above and Below Ground. *Environ. Sci. Technol.* **2019**, 53 (19), 11496–11506.
- (7) Franzellitti, S.; Canesi, L.; Auguste, M.; Wathsala, R. H. G. R.; Fabbri, E. Microplastic Exposure and Effects in Aquatic Organisms: A Physiological Perspective. *Environ. Toxicol. Pharmacol.* **2019**, *68*, 37–51.
- (8) Mohsin, M. A.; Abdulrehman, T.; Haik, Y. Reactive Extrusion of Polyethylene Terephthalate Waste and Investigation of Its Thermal and Mechanical Properties after Treatment. *Int. J. Chem. Eng.* **2017**, 2017, No. 5361251.
- (9) Zhao, Y.-B.; Lv, X.-D.; Ni, H.-G. Solvent-Based Separation and Recycling of Waste Plastics: A Review. *Chemosphere* **2018**, 209, 707–720.
- (10) Jehanno, C.; Alty, J. W.; Roosen, M.; De Meester, S.; Dove, A. P.; Chen, E. Y.-X.; Leibfarth, F. A.; Sardon, H. Critical Advances and Future Opportunities in Upcycling Commodity Polymers. *Nature* **2022**, *603* (7903), 803–814.
- (11) Maafa, I. M. Pyrolysis of Polystyrene Waste: A Review. *Polymers* **2021**, *13* (2), No. 225.

- (12) Ügdüler, S.; Van Geem, K. M.; Roosen, M.; Delbeke, E. I. P.; De Meester, S. Challenges and Opportunities of Solvent-Based Additive Extraction Methods for Plastic Recycling. *Waste Manage*. **2020**, *104*, 148–182.
- (13) Dutt, K.; Soni, R. K. Synthesis and Characterization of Polymeric Plasticizer from PET Waste and Its Applications in Nitrile Rubber and Nitrile—PVC Blend. *Iran. Polym. J.* **2013**, 22 (7), 481–491.
- (14) Chiaie, K. R. D.; McMahon, F. R.; Williams, E. J.; Price, M. J.; Dove, A. P. Dual-Catalytic Depolymerization of Polyethylene Terephthalate (PET). *Polym. Chem.* **2020**, *11* (8), 1450–1453.
- (15) Fukushima, K.; Coulembier, O.; Lecuyer, J. M.; Almegren, H. A.; Alabdulrahman, A. M.; Alsewailem, F. D.; Mcneil, M. A.; Dubois, P.; Waymouth, R. M.; Horn, H. W.; Rice, J. E.; Hedrick, J. L. Organocatalytic Depolymerization of Poly(Ethylene Terephthalate): Organocatalytic Depolymerization of Pet. J. Polym. Sci., Part A: Polym. Chem. 2011, 49 (5), 1273–1281.
- (16) US is Creating More Plastic Waste and Recycling Less of it I World Economic Forum 2023. https://www.weforum.org/agenda/2022/05/plastic-waste-generation-new-highs-us-report/#:%7E:text=The%20plastic%20recycling%20rate%20is,and%20Turkey%20ban ning%20such%. (accessed December 18, 2023).
- (17) Holmberg, A. L.; Reno, K. H.; Wool, R. P.; Epps, T. H., III Biobased Building Blocks for the Rational Design of Renewable Block Polymers. *Soft Matter* **2014**, *10* (38), 7405–7424.
- (18) Ma, S.; Wei, J.; Jia, Z.; Yu, T.; Yuan, W.; Li, Q.; Wang, S.; You, S.; Liu, R.; Zhu, J. Readily Recyclable, High-Performance Thermosetting Materials Based on a Lignin-Derived Spiro Diacetal Trigger. *J. Mater. Chem. A* **2019**, *7* (3), 1233–1243.
- (19) Van Zee, N. J.; Coates, G. W. Alternating Copolymerization of Propylene Oxide with Biorenewable Terpene-Based Cyclic Anhydrides: A Sustainable Route to Aliphatic Polyesters with High Glass Transition Temperatures. *Angew. Chem., Int. Ed.* **2015**, *54* (9), 2665–2668.
- (20) Suyatma, N. E.; Copinet, A.; Tighzert, L.; Coma, V. Mechanical and Barrier Properties of Biodegradable Films Made from Chitosan and Poly (Lactic Acid) Blends. *J. Polym. Environ.* **2004**, *12* (1), 1–6.
- (21) Sangroniz, A.; Zhu, J.-B.; Tang, X.; Etxeberria, A.; Chen, E. Y.-X.; Sardon, H. Packaging Materials with Desired Mechanical and Barrier Properties and Full Chemical Recyclability. *Nat. Commun.* **2019**, *10* (1), No. 3559.
- (22) Sid, S.; Mor, R. S.; Kishore, A.; Sharanagat, V. S. Bio-Sourced Polymers as Alternatives to Conventional Food Packaging Materials: A Review. *Trends Food Sci. Technol.* **2021**, *115*, 87–104.
- (23) Erlandsson, B.; Karlsson, S.; Albertsson, A.-C. The Mode of Action of Corn Starch and a Pro-Oxidant System in LDPE: Influence of Thermo-Oxidation and UV-Irradiation on the Molecular Weight Changes. *Polym. Degrad. Stab.* **1997**, *55*, 237–245.
- (24) Huang, J.-C.; Shetty, A. S.; Wang, M.-S. Biodegradable Plastics: A Review. *Adv. Polym. Technol.* **1990**, *10* (1), 23–30.
- (25) Selke, S.; Auras, R.; Nguyen, T. A.; Aguirre, E. C.; Cheruvathur, R.; Liu, Y. Evaluation of Biodegradation-Promoting Additives for Plastics. *Environ. Sci. Technol.* **2015**, 49 (6), 3769–3777.
- (26) Ilyas, R. A.; Sapuan, S. M.; Ishak, M. R.; Zainudin, E. S.; Atikah, M. S. N.; Huzaifah, M. R. M. Water Barrier Properties of Biodegradable Films Reinforced with Nanocellulose for Food Packaging Application: A Review, 6th Postgraduate Seminar on Natural Fiber Reinforced Polymer Composites; Institute of Tropical Forestry and Forest Product (INTROP), Universiti Putra Malaysia, 2018.
- (27) Dimiev, A. M.; Alemany, L. B.; Tour, J. M. Graphene Oxide. Origin of Acidity, Its Instability in Water, and a New Dynamic Structural Model. *ACS Nano* **2013**, *7* (1), 576–588.
- (28) Holt, B. D.; Arnold, A. M.; Sydlik, S. A. In It for the Long Haul: The Cytocompatibility of Aged Graphene Oxide and Its Degradation Products. *Adv. Healthcare Mater.* **2016**, *5* (23), 3056–3066.
- (29) Su, Y.; Kravets, V. G.; Wong, S. L.; Waters, J.; Geim, A. K.; Nair, R. R. Impermeable Barrier Films and Protective Coatings Based on Reduced Graphene Oxide. *Nat. Commun.* **2014**, *5* (1), No. 4843.

- (30) Ren, P.-G.; Liu, X.-H.; Ren, F.; Zhong, G.-J.; Ji, X.; Xu, L. Biodegradable Graphene Oxide Nanosheets/Poly-(Butylene Adipate-Co-Terephthalate) Nanocomposite Film with Enhanced Gas and Water Vapor Barrier Properties. *Polym. Test.* **2017**, *58*, 173–180.
- (31) Yousefi, N.; Gudarzi, M. M.; Zheng, Q.; Lin, X.; Shen, X.; Jia, J.; Sharif, F.; Kim, J.-K. Highly Aligned, Ultralarge-Size Reduced Graphene Oxide/Polyurethane Nanocomposites: Mechanical Properties and Moisture Permeability. *Composites, Part A* **2013**, *49*, 42–50.
- (32) Tarhini, A.; Tehrani-Bagha, A.; Kazan, M.; Grady, B. The Effect of Graphene Flake Size on the Properties of Graphene-Based Polymer Composite Films. *J. Appl. Polym. Sci.* **2021**, *138* (6), No. 49821.
- (33) Papageorgiou, D. G.; Kinloch, I. A.; Young, R. J. Mechanical Properties of Graphene and Graphene-Based Nanocomposites. *Prog. Mater. Sci.* **2017**, *90*, 75–127.
- (34) Dai, Z.; Wang, G.; Liu, L.; Hou, Y.; Wei, Y.; Zhang, Z. Mechanical Behavior and Properties of Hydrogen Bonded Graphene/Polymer Nano-Interfaces. *Compos. Sci. Technol.* **2016**, *136*, 1–9.
- (35) Paschke, E. E.; Bidlingmeyer, B. A.; Bergmann, J. G. A New Solvent System for Gel-Permeation Chromatography of Poly-(Ethylene Terephthalate). *J. Polym. Sci., Polym. Chem. Ed.* 1977, 15 (4), 983–989.
- (36) Yang, W.; Wang, J.; Jiao, L.; Song, Y.; Li, C.; Hu, C. Easily Recoverable and Reusable *p* -Toluenesulfonic Acid for Faster Hydrolysis of Waste Polyethylene Terephthalate. *Green Chem.* **2022**, 24 (3), 1362–1372.
- (37) Stanica-Ezeanu, D.; Matei, D. Natural Depolymerization of Waste Poly(Ethylene Terephthalate) by Neutral Hydrolysis in Marine Water. *Sci. Rep.* **2021**, *11* (1), No. 4431.
- (38) Arias, J. J. R.; Thielemans, W. Instantaneous Hydrolysis of PET Bottles: An Efficient Pathway for the Chemical Recycling of Condensation Polymers. *Green Chem.* **2021**, 23 (24), 9945–9956.
- (39) Coltelli, M.-B.; Toncelli, C.; Ciardelli, F.; Bronco, S. Compatible Blends of Biorelated Polyesters through Catalytic Transesterification in the Melt. *Polym. Degrad. Stab.* **2011**, *96* (5), 982–990.
- (40) Wang, L.-H.; Huang, Z.; Hong, T.; Porter, R. S. The Compatibility and Transesterification for Blends of Polyethylene Terephthalate)/Poly(Bisphenol-A Carbonate). *J. Macromol. Sci., Part B* **1990**, 29 (2–3), 155–169.
- (41) Fukushima, K.; Coady, D. J.; Jones, G. O.; Almegren, H. A.; Alabdulrahman, A. M.; Alsewailem, F. D.; Horn, H. W.; Rice, J. E.; Hedrick, J. L. Unexpected Efficiency of Cyclic Amidine Catalysts in Depolymerizing Poly(Ethylene Terephthalate). *J. Polym. Sci., Part A: Polym. Chem.* **2013**, *51* (7), 1606–1611.
- (42) Korshak, V. V.; Zamyatina, V. A.; Bekasova, N. I.; Oganesyan, R. M.; Solomatina, A. I. Boric Polyesters. *Bull. Acad. Sci. USSR, Div. Chem. Sci.* 1963, 12, 1496–1502.
- (43) Halacheva, N.; Novakov, P. Preparation of Oligoester Diols by Alcoholytic Destruction of Poly(Ethylene Terephthalate). *Polymer* **1995**, *36* (4), 867–874.
- (44) Ramesh, P.; Bhagyalakshmi, S.; Sampath, S. Preparation and Physicochemical and Electrochemical Characterization of Exfoliated Graphite Oxide. *J. Colloid Interface Sci.* **2004**, *274* (1), 95–102.
- (45) Eckhart, K. E.; Holt, B. D.; Laurencin, M. G.; Sydlik, S. A. Covalent Conjugation of Bioactive Peptides to Graphene Oxide for Biomedical Applications. *Biomater. Sci.* **2019**, *7* (9), 3876–3885.
- (46) Zhang, H.-B.; Feng, R.-J.; Ura, K. Utilizing the Charging Effect in Scanning Electron Microscopy. *Sci. Prog.* **2004**, *87* (4), 249–268.
- (47) Grewell, D.; Srinivasan, G.; Cochran, E. Depolymerization of Post-Consumer Polylactic Acid Products. *J. Renewable Mater.* **2014**, 2 (3), 157–165.
- (48) Zhu, C.; Fan, C.; Hao, Z.; Jiang, W.; Zhang, L.; Zeng, G.; Sun, P.; Zhang, Q. Molecular Mechanism of Waste Polyethylene Terephthalate Recycling by the 1,5,7-Triazabicyclo[4.4.0]Decium Acetate/ Zinc Acetate Deep Eutectic Solvent: The Crucial Role of 1,5,7-Triazabicyclo[4.4.0]Decium Cation. *Appl. Catal., A* 2022, 641, No. 118681.

- (49) Raux, P. S.; Gravelle, S.; Dumais, J.; et al. Design of a Unidirectional Water Valve in Tillandsia. *Nat. Commun.* **2020**, *11*, No. 396
- (50) Keller, P. E.; Kouzes, R. T. Water Vapor Permeation in Plastics; Pacific Northwest National Lab, 2017.
- (51) Nair, R. R.; Wu, H. A.; Jayaram, P. N.; Grigorieva, I. V.; Geim, A. K. Unimpeded Permeation of Water Through Helium-Leak—Tight Graphene-Based Membranes. *Science* **2012**, 335 (6067), 442–444.
- (52) Joshi, R. K.; Carbone, P.; Wang, F. C.; Kravets, V. G.; Su, Y.; Grigorieva, I. V.; Wu, H. A.; Geim, A. K.; Nair, R. R. Precise and Ultrafast Molecular Sieving Through Graphene Oxide Membranes. *Science* **2014**, 343 (6172), 752–754.
- (53) Tasić, Z. Z.; Mihajlović, M. B. P.; Simonović, A. T.; Radovanović, M. B.; Antonijević, M. M. Ibuprofen as a Corrosion Inhibitor for Copper in Synthetic Acid Rain Solution. *Sci. Rep.* **2019**, 9 (1), No. 14710.
- (54) Practice for the Preparation of Substitute Ocean Water; ASTM International, 2022.
- (55) Mechanics of Composite Materials; Wendt, F. W.; Liebowitz, H.; Perrone, N., Eds.; Elsevier, 1970.
- (56) Kar, G. P.; Biswas, S.; Bose, S. Tailoring the Interface of an Immiscible Polymer Blend by a Mutually Miscible Homopolymer Grafted onto Graphene Oxide: Outstanding Mechanical Properties. *Phys. Chem. Chem. Phys.* **2015**, *17* (3), 1811–1821.
- (57) Zhang, C.; Li, T.; Song, H.; Han, Y.; Dong, Y.; Wang, Y.; Wang, Q. Improving the Thermal Conductivity and Mechanical Property of Epoxy Composites by Introducing Polyhedral Oligomeric Silsesquioxane-Grafted Graphene Oxide. *Polym. Compos.* **2018**, 39 (S3), E1890–E1899.
- (58) Katti, P.; Kundan, K. V.; Kumar, S.; Bose, S. Improved Mechanical Properties through Engineering the Interface by Poly (Ether Ether Ketone) Grafted Graphene Oxide in Epoxy Based Nanocomposites. *Polymer* **2017**, *122*, 184–193.
- (59) Liu, K.; Chen, L.; Chen, Y.; Wu, J.; Zhang, W.; Chen, F.; Fu, Q. Preparation of Polyester/Reduced Graphene Oxide Composites via in Situ Melt Polycondensation and Simultaneous Thermo-Reduction of Graphene Oxide. *J. Mater. Chem.* **2011**, *21* (24), 8612.
- (60) Xia, W.; Yang, J.; Liang, C. Investigation of Changes in Surface Properties of Bituminous Coal during Natural Weathering Processes by XPS and SEM. *Appl. Surf. Sci.* **2014**, 293, 293–298.
- (61) Hongjuan, S.; Tongjiang, P.; Bo, L.; Caifeng, M.; Liming, L.; Quanjun, W.; Jiaqi, D.; Xiaoyi, L. Study of Oxidation Process Occurring in Natural Graphite Deposits. *RSC Adv.* **2017**, *7* (81), 51411–51418.
- (62) Yang, W.; Liu, R.; Li, C.; Song, Y.; Hu, C. Hydrolysis of Waste Polyethylene Terephthalate Catalyzed by Easily Recyclable Terephthalic Acid. *Waste Manage.* **2021**, *135*, 267–274.
- (63) Wu, G.; McHugh, E. A.; Berka, V.; Chen, W.; Wang, Z.; Beckham, J. L.; Derry, P. J.; Roy, T.; Kent, T. A.; Tour, J. M.; Tsai, A.-L. Oxidized Activated Charcoal Nanoparticles as Catalytic Superoxide Dismutase Mimetics: Evidence for Direct Participation of an Intrinsic Radical. ACS Appl. Nano Mater. 2020, 3 (7), 6962–6971.

Recommended by ACS

HydrothPerromocaelos 15Miu In by i Pla ay £e **trifoo**r Casc aVdael dor ioz Naotriro enc yWdalsatbel e

Ran Darzi, RoyaPosmanik, DECEMBER 11, 2023 ACS SUSTAINABLE CHEMISTRY & ENGINEERRFMAST

PreparoaGtrieœenna Lode gra of Sae ba lwa®s e sl Se tdra ws byDirec DiofinaAlssis oe ma baalPyla Situbs titute

Yuanpu Liu,e Feagwei Xie, OCTOBER 30, 2023 ACS SUSTAINABLE CHEMISTRY & ENGINEE**R**FMAST<mark>A</mark>

Fro Whas **t** 6 il a:mDeenvte loop Bene on th-Dasis ived ActivCaatreb-Boenin f B E T: 6 of mposiotres Sustai3 nDParbilnet in g

Salar Balou, etA aashish Priye, AUGUST 14, 2023 ACS SUSTAINABLE CHEMISTRY & ENGINEER ENAIS

Cell Miliocs of greigh eonSitmagNahocomposites ExplotihtAeidnvoan toat/tijecsNaonosNceatlvoeorks

Bin Sun, etQiaIZ.hou, OCTOBER 16, 2023

ACS SUSTAINABLE CHEMISTRY & ENGINEER ENAM

Get More Suggestions >